Advances in Physics Theories and Applications
ISSN 2224-719X (Paper) ISSN 2225-0638 (Online)
Vol.26, 2013

The Effect of Soot and Water Soluble on the Hygroscopicity of Urban Aerosols

B. I. Tijjani
Department of Physics, Bayero University, Kano. NIGERIA.
Emails: idrith@yahoo.com, idrithtijjani@gmail.com

ABSTRACT

In this paper, the author investigated some microphysical and optical properties of urban aerosols from OPAC by varying the concentrations of soot and water soluble to determine the effect of hygroscopic growth at the spectral range of 0.25μm to 2.5μm and eight relative humidities (RHs) (0, 50, 70, 80, 90, 95, 98, and 99%).The microphysical properties extracted were radii, volume mix ratio, number mix ratio, mass mix ratio and refractive indices while the optical properties are optical depth and asymmetric parameters all as a function of RHs. Using the microphysical properties, hygroscopic growth factors of the mixtures were determined while using optical depths we determined the Angstrom coefficients, enhancement parameters and the relationship between optical depth and RHs. The growth factors and the enhancement parameters were then parameterized using some models to determine their relationships with RHs. The data fitted the models very well. The angstrom coefficients show that the mixture have bimodal type of distribution with the dominance of fine mode particles and the mode sizes increase with the increase in RH and soot and water soluble concentrations.

Keywords: microphysical properties, optical properties, hygroscopic growth, enhancement parameter, spectral range, Angstrom coefficients, bimodal.

INTRODUCTION

Atmospheric aerosols are complex in their sources, evolution, and interactions with water vapor in the atmosphere and they influence the climate directly by absorbing as well as reflecting the incoming short-wave solar radiation back to space. Hygroscopicity (i.e. water vapour affinity) of atmospheric aerosol particles is one of the key factors in defining their impacts on climate. These aerosol particles reveal changes in their microphysical and optical properties with relative humidity (RH) due to the water uptake. These changes depend on the particles' chemical composition, size and the ambient relative humidity (RH) [1-3]. Depending on the chemical compositions, aerosol particles can take up large amounts of water compared to their dry state as relative humidity (RH) increases and this can radically increase their sizes cause changes in the effective indices and their optical properties [4].

In the natural environments the changes in the microphysical and optical properties observed at a given wavelength are signs that measuring conditions have changed. These changes can be related either to an increase in RH or to a change in the aerosol concentration. Quite often, both factors are present. Optical measurements at one single wavelength will not resolve the question whether the observed changes are caused only by the increased humidity or whether the additional aerosol particles have contributed to the measured aerosol optical properties. To be able to retrieve more accurate information about an aerosol mixture, spectral measurements are needed. The more spectral information available, the greater are the chances of getting a more realistic idea of the aerosol composition.

Furthermore, cloud droplets and water in deliquesced aerosol particles provide an aqueous medium for chemical reactions, which can lead to a change in the chemical composition of the particles [5-9]. As the ambient relative humidity (RH) changes, hygroscopic atmospheric aerosols undergo phase transformation, droplet growth, and evaporation. Phase transformation from a solid particle to a saline droplet usually occurs spontaneously when the RH reaches a level called the deliquescence humidity. Its value is specific to the chemical composition of the aerosol particle [10,11]. Since aerosols are far from being a single component, the question is how relative humidity influences the optical properties of natural aerosol mixtures, which can contain both soluble and insoluble components. Most atmospheric aerosols are externally mixed with respect to hygroscopicity, and consist of more and less hygroscopic sub-fractions [12]. The ratio between these fractions as well as their content of soluble material determines the hygroscopic growth of the overall aerosol. To model droplet growth, information about water activity and density as a function of solute concentrations is needed. The chemical and physical characteristics of aerosols are diverse and attempting to encompass such variability within a hygroscopic model is complex. An aerosol may exist in a solid or liquid state or a combination of the two over a wide range of ambient conditions both in the sub and super saturated humid environment [13-16]. Thus, where

possible, the ability to couple the chemical and physical characteristics to the equilibrium phase of the aerosol is the ultimate aim of any hygroscopic modeling approach. Indeed, Martin et al. [17] found that direct radiative forcing estimates were particularly sensitive to the predicted physical state of the aerosol.

On a global basis, sulfates, nitrates and chlorides contribute the largest to the mass budget of fine atmospheric particles [18-20]. These inorganic salt aerosols are hygroscopic by nature, thus their size, phase and subsequently the optical properties would be strongly influenced by the ambient relative humidity (RH). Hand and Malm [21] indicated that the scattering coefficients of $(NH_4)_2SO_4$ and $(NH_4)HSO_4$ aerosols could be enhanced by a factor of three when relative humidity is over 85%. Based on recent studies, close attention has been paid to study the hygroscopic properties of these inorganic salts, because the effect of sulfate particles on the annual-average global direct radiative forcing, arising from the fluctuation of atmospheric particles between aqueous and solid state, is estimated up to as much as 24% [17,22,23]. Soot aerosols produced from fossil-fuel combustion, automobile and aircraft emissions, and biomass burning are ubiquitous in the atmosphere, comprising10–50% of the total tropospheric particulate matter [24-29]. Once emitted into the atmosphere, soot particles are subjected to several aging processes, coagulation with other preexisting aerosols, and oxidation [14,16,30]. Model calculations have shown that, when associated with other very hygroscopic aerosol constituents (e.g., sulfate), soot seems more absorptive and exerts a higher positive direct radiative forcing, and the warming effect by soot nearly balances the net cooling effect of other anthropogenic aerosols [28,31].

The hygroscopicity of aerosols are currently modeled in global climate models (GCMs), mostly to better predict the scattering properties and size distribution under varying humidity conditions and concentrations [32]. The mixing state and associated physical, optical, and geometrical properties of soot particles are of critical importance in evaluating the effects of light-absorbing aerosols and improving climate predictions by using global climate models (GCMs).

The main parameters used to characterize the hygroscopicity of the aerosol particles are the aerosol hygroscopic growth factor of the mixtures ($gf_{mix}(RH)$) [12,33-39].

Measured and modeled enhancement factors have been described in several previous studies, including studies on urban [40,41].

Jeong et al. [42] demonstrated an exponential dependence of the aerosol optical thickness on relative humidity. A strong correlation of spectral aerosol optical thickness with precipitable water, especially for continental air masses, was shown by Rapti [43].

In this paper some microphysical and optical properties of urban aerosols were extracted from OPAC at the spectral wavelength of 0.25 to 2.50μm, at relative humidities of 0, 50, 70, 80, 90, 95, 98 and 99% and varying the concentrations of soot and water soluble. The microphysical properties extracted are diameters of the aerosols, number mix ratios, volume mix ratio, mass mix ratio and refractive indices. They were used to determine the hygroscopic growth and the effective refractive indices of the mixtures. The optical depths were used to determine the angstrom parameters using power law and enhancement parameters. The angstrom coefficients were used to determine the particles' type and the type mode size distributions. One and two parameter models were used to determine the relationship between the enhancement parameters and hygroscopic growths with RHs. The asymmetric parameters were used to determine the effects of hygroscopic growth on forward scattering.

METHODOLOGY

Table 1: Compositions of aerosols types [44].

Components	ModelA (N_i,cm^{-3})	ModelB (N_i,cm^{-3})	ModelC (N_i,cm^{-3})
water insoluble	1.5	1.5	1.5
water soluble	20,000.0	25,000.0	30,000.0
Soot	110,000.0	120,000.0	130,000.0
Total	130,001.5	145,001.5	160,001.5

Where (N_i,cm^{-3}) is the number of particles cm^{-3}, water soluble components , consist of scattering aerosols, that are hygroscopic in nature, such as sulfates and nitrates present in anthropogenic pollution, while water insoluble and soot are considered not soluble in water and therefore the particles are assumed not to grow with increasing relative humidity.
The aerosol's hygroscopic growth factor gf(RH), [12,45] is defined as:

$$gf(RH) = \frac{D(RH)}{D(RH=0)} \quad (1)$$

where RH is taken for seven values 50%, 70%, 80%, 90%, 95%, 98% and 99%. But since natural aerosols consist of mixtures of both the soluble and insoluble components, and more and less hygroscopic sub fractions, so information on the hygroscopicity modes was merged into an "over-all" hygroscopic growth factor of the mixture, $gf_{mix}(RH)$, representative for the entire particle population as:

$$gf_{mix}(RH) = (\sum_k x_k gf_k^3)^{1/3} \quad (2)$$

where the summation is performed over all compounds present in the particles and x_k represent their respective volume fractions, using the Zdanovskii-Stokes-Robinson relation [46-49]. Solute-solute interactions are neglected in this model and volume additivity is also assumed. The model assumes spherical particles, ideal mixing (i.e. no volume change upon mixing) and independent water uptake of the components.

Equation (2) was also computed using the x_k as the corresponding number fractions [50,51].

We finally proposed the x_k to represent the mass mix ratio of the individual particles, but since mass and volume are proportional, this will enable us to see the effect of hygroscopic growth on the density of the mixture.

The RH dependence of $gf_{mix}(RH)$ was parameterized in a good approximation by a one-parameter equation, Petters and Kreidenweis [52] as:

$$gf_{mix}(a_w) = \left(1 + \kappa \frac{a_w}{1-a_w}\right)^{\frac{1}{3}} \quad (3)$$

Here, a_w is the water activity, which can be replaced by the relative humidity RH, if the Kelvin effect is negligible, as for particles with sizes more relevant for light scattering and absorption. Particle hygroscopicity is a measure that scales the volume of water associated with a unit volume of dry particle [52] and depends on the molar volume and the activity coefficients of the dissolved compounds [53]. The coefficient κ is a simple measure of the particles' hygroscopicity and captures all solute properties (Raoult effect), that is it is for the ensemble of the particle which can be defined in terms of the sum of its components. The κ value derived a particle of a given composition may vary, depending upon the size and RH it is derived at. Nearly-hydrophobic particles (NH): κ<=0.10 (gf_{mix}<=1.21), less-hygroscopic particles (LH): κ=0.10 – 0.20 (gf_{mix} =1.21 – 1.37); more-hygroscopic particles (MH): κ>0.20 (gf_{mix} >1.37) [54].

Humidograms of the ambient aerosols obtained in various atmospheric conditions showed that $gf_{mix}(RH)$ could as well be fitted well with a γ-law [55-59] as

$$gf_{mix}(RH) = \left(1 - \frac{RH}{100}\right)^{\gamma} \quad (4)$$

The bulk hygroscopicity factor B under subsaturation RH conditions was determined using the relation:

$$B = (1 - gf_{mix}^3)\ln a_w \quad (5)$$

where a_w is the water activity, which can be replaced by the RH as explained before. Equation(5) can be described as the rate of absorption of water of the bulk mixture as the RH increases.

The impact of hygroscopic growth on the aerosol optical depth is usually described by the enhancement factor $f_\tau(RH,\lambda)$:

$$f_\tau(RH,\lambda) = \frac{\tau(RH,\lambda)}{\tau(RH=0,\lambda)} \quad (6)$$

where RH is taken for seven values 50, 70, 80, 90, 95, 98 and 99%.

In general the relationship between $f_\tau(RH,\lambda)$ and RH is nonlinear [42]. In this paper we determined the empirical relations between the enhancement parameter and RH [60] as:

$$f_\tau(RH,\lambda) = \frac{\tau(RH,\lambda)}{\tau(RH_{ref},\lambda)} = \left(\frac{100-RH_{ref}}{100-RH_{high}}\right)^{\gamma} \quad (7)$$

where in our study RH_{ref} was 0%, and RH_{high} were taken for seven values 50%, 70%, 80%, 90%, 95%, 98% and 99%. The γ known as the humidification factor represents the dependence of aerosol optical properties on RH, which results from changes in the particle size and refractive index upon humidification. The use of γ has the advantage of describing the hygroscopic behavior of aerosols in a linear manner over a broad range of RH values; it also implies that particles are deliquesced [61], a reasonable assumption for this data set due to the high ambient relative humidity during the field study. The γ parameter is dimensionless, and it increases with increasing particle water uptake. From previous studies, typical values of γ for ambient aerosol ranged between 0.1 and 1.5 [61-63].

Two parameters empirical relation was used [42,64] as;

$$f_\tau(RH,\lambda) = a\left(1-\frac{RH(\%)}{100}\right)^{b} \quad (8)$$

Equations (7) and (8) are verified at wavelengths 0.25, 0.45, 0.55, 0.70, 1.25, and 2.50μm.

To determine the effect of particles distributions as a result of change in RH and change in aerosols concentrations, the Angstrom exponent was determined using the spectral behavior of the aerosol optical depth, with the wavelength of light (λ) expressed as inverse power law [65]:

$$\tau(\lambda) = \beta\lambda^{-\alpha} \quad (9)$$

The Angstrom exponent was obtained as a coefficient of the following regression,

$$\ln\tau(\lambda) = -\alpha\ln(\lambda) + \ln\beta \quad (10)$$

However equation (10) was determined as non-linear (that is the Angstrom exponent itself varies with wavelength), and a more precise empirical relationship between the optical depth and wavelength was obtained with a 2nd-order polynomial [66-76] as:

$$\ln\tau(\lambda)=\alpha_2(\ln\lambda)^2 + \alpha_1\ln\lambda + \ln\beta \quad (11)$$

We then proposed the cubic relation to determine the type of mode distribution as:

$$\ln X(\lambda)= \ln\beta + \alpha_1\ln\lambda + \alpha_2(\ln\lambda)^2+ \alpha_3(\ln\lambda)^3 \quad (12)$$

where β, α, α_1, α_2, α_3 are constants that were determined using regression analysis with SPSS16.0.

We also determined an exponential dependence of the aerosol optical thickness on relative humidity as done by Jeong et al. [42] as;

$$\tau(RH) = Ae^{B(RH/100)} \quad (13)$$

where A and B are constants determined using regression analysis with SPSS 16.0. for windows.

We finally determine the effect of hygroscopic growth and change in the change in the concentration of soot and water soluble on the effective refractive indices of the mixed aerosols using the following formula [77]:

$$\frac{\varepsilon_{eff}-\varepsilon_0}{\varepsilon_{eff}+2\varepsilon_0} = \sum_{j=1}^{j} f_j \frac{\varepsilon_j-\varepsilon_0}{\varepsilon_j+2\varepsilon_0} \quad (14)$$

where f_i and ε_i are the volume fraction and dielectric constant of the i^{th} component and ε_0 is the dielectric constant of the host material.

The relation between dielectrics and refractive indices is

$$m_j = \sqrt{\varepsilon_j} \quad (15)$$

For the case of Lorentz-Lorentz [77-78], the host material is taken to be vacuum, ε_0 =1.

The computations of equations(14) and (15) were performed using the complex functions of Microsoft Excel 2010.

RESULTS AND DISCUSSIONS

Table 2a: the growth factor of the aerosols using number mix ratio (equation 2) and Bulk hygroscopicity factor (equation 5) for Model A.

RH(%)	50	70	80	90	95	98	99
$gf_{mix}(RH)$	1.0435	1.0685	1.0938	1.1514	1.2323	1.3728	1.4894
B	0.0946	0.0784	0.0689	0.0555	0.0447	0.0321	0.0232

Table 2b: the growth factor of the aerosols using number mix ratio (equation 2) and Bulk hygroscopicity factor (equation 5) for Model B.

RH(%)	50	70	80	90	95	98	99
$gf_{mix}(RH)$	1.0486	1.0762	1.1041	1.1672	1.2551	1.4059	1.5302
B	0.1061	0.0879	0.0772	0.0622	0.0501	0.0359	0.0260

Table 2c: the growth factor of the aerosols using number mix ratio (equation 2) and Bulk hygroscopicity factor (equation 5) for Model C.

RH(%)	50	70	80	90	95	98	99
$gf_{mix}(RH)$	1.0527	1.0824	1.1124	1.1797	1.2729	1.4317	1.5617
B	0.1154	0.0956	0.0840	0.0676	0.0545	0.0391	0.0282

From tables 2a, 2b and 2c it can be seen that there is an increase in both $gf_{mix}(RH)$ and B with the increase in the concentrations of soot and water soluble. It can also be observed that hygroscopic growth has caused increased in $gf_{mix}(RH)$ but decrease in B.

The data from tables 2a, 2b and 2c were applied for the parametrisations of equations (3) and (4). The results obtained are as follows:

The results of the parameterizations by one parameter of equations (3) and (4) for ModelA using number mix ratio are:

k= 0.0260, R2= 0.9470 (from equation 3)

γ= -0.0773 , R2= 0.9824 (from equation 4)

The results of the parameterizations by one parameter of equations (3) and (4) for Model B using number mix ratio are:

k= 0.0291, R2= 0.9470 (from equation 3)

γ= -0.0833 , R2= 0.9849 (from equation 4)

The results of the parameterizations by one parameter of equations (3) and (4) for Model C using number mix ratio are:

k= 0.0317, R2= 0.9470 (from equation 3)

γ= -0.0879 , R2= 0.9866 (from equation 4)

From the results of the parametrisation of $gf_{mix}(RH)$ and RH using equations (3) and (4) on the data of tables 2a, 2b and 2c, it can be seen that the data fitted the equations very well because of the values of R^2. It can also be observed that hygroscopicity of the mixtures (k) and γ using γ-law, all increase with the increase in the

concentrations of the soots and the water solubles. Based on Liu et. al., [54] the mixtures can be described as nearly-hygroscopic.

Table 3a: the growth factor of the aerosols using volume mix ratio (equation 2) and Bulk hygroscopicity factor (equation 5) for Model A.

RH(%)	50	70	80	90	95	98	99
$gf_{mix}(RH)$	1.1384	1.2286	1.3200	1.5181	1.7706	2.1556	2.4435
B	0.3296	0.3047	0.2901	0.2633	0.2334	0.1821	0.1366

Table 3b: the growth factor of the aerosols using volume mix ratio (equation 2) and Bulk hygroscopicity factor (equation 5) for Model B.

RH(%)	50	70	80	90	95	98	99
$gf_{mix}(RH)$	1.1495	1.2432	1.3367	1.5364	1.7882	2.1706	2.4564
B	0.3597	0.3286	0.3098	0.2768	0.2420	0.1864	0.1389

Table 3c: the growth factor of the aerosols using volume mix ratio (equation 2) and Bulk hygroscopicity factor (equation 5) for Model C.

RH(%)	50	70	80	90	95	98	99
$gf_{mix}(RH)$	1.1579	1.2540	1.3488	1.5494	1.8005	2.1808	2.4652
B	0.3830	0.3467	0.3244	0.2865	0.2481	0.1893	0.1405

From tables 3a, 3b and 3c it can be seen that there is an increase in both $gf_{mix}(RH)$ and B with the increase in the concentrations of soot and water soluble. It can also be observed the hygroscopic growth has caused increased in $gf_{mix}(RH)$ but decrease in B.

The data from tables 3a, 3b and 3c were applied for the parametrisations of equations (3) and (4). The results obtained are as follows:

The results of the parameterizations by one parameter of equations (3) and (4) for ModelA using volume mix ratio are:

k= 0.1503, R2= 0.9681 (from equation 3)

γ= -0.1912 , R2= 0.9987 (from equation 4)

The results of the parameterizations by one parameter of equations (3) and (4) for Model B using volume mix ratio are:

k= 0.1533 , R2= 0.9655 (from equation 3)

γ= -0.1939, R2= 0.9994 (from equation 4)

The results of the parameterizations by one parameter of equations (3) and (4) for Model C using volume mix ratio are:

k= 0.1554 , R2= 0.9635 (from equation 3)

γ= -0.1958 , R2= 0.9996 (from equation 4)

From the results of the parametrisation of $gf_{mix}(RH)$ and RH using equations (3) and (4) on the data of tables 3a, 3b and 3c, it can be seen that the data fitted the equations very well because of the values of R^2. It can also be observed that hygroscopicity of the mixtures (k) and γ using γ-law, all increase with the increase in the concentrations of the soots and the water solubles. Based on Liu et. al., [54] the mixtures can be described as less-hygroscopic.

Table 4a: the growth factor of the aerosols using mass mix ratio (equation 2) and Bulk hygroscopicity factor (equation 5) for Model A.

RH(%)	50	70	80	90	95	98	99
$gf_{mix}(RH)$	1.1271	1.2078	1.2912	1.4766	1.7224	2.1078	2.3997
B	0.2992	0.2718	0.2573	0.2338	0.2108	0.1690	0.1288

Table 4b: the growth factor of the aerosols using mass mix ratio (equation 2) and Bulk hygroscopicity factor (equation 5) for Model B.

RH(%)	50	70	80	90	95	98	99
$gf_{mix}(RH)$	1.1391	1.2244	1.3110	1.5004	1.7472	2.1308	2.4203
B	0.3314	0.2981	0.2797	0.2505	0.2223	0.1752	0.1324

Table 4c: the growth factor of the aerosols using mass mix ratio (equation 2) and Bulk hygroscopicity factor (equation 5) for Model C.

RH(%)	50	70	80	90	95	98	99
$gf_{mix}(RH)$	1.1485	1.2371	1.3259	1.5176	1.7650	2.1468	2.4345
B	0.3569	0.3186	0.2970	0.2629	0.2307	0.1797	0.1350

From tables 4a, 4b and 4c it can be seen that there is an increase in both $gf_{mix}(RH)$ and B with the increase in the concentrations of soot and water soluble. It can also be observed the hygroscopic growth has caused increased in $gf_{mix}(RH)$ but decrease in B.

The data from tables 4a, 4b and 4c were applied for the parametrisations of equations (3) and (4). The results obtained are as follows:

The results of the parameterizations by one parameter of equations (3) and (4) for ModelA using mass mix ratio are:

k= 0.1408, R^2= 0.9729 (from equation 3)

γ= -0.1844 , R^2= 0.9971 (from equation 4)

The results of the parameterizations by one parameter of equations (3) and (4) for Model B using mass mix ratio are:

k= 0.1453, R^2= 0.9699 (from equation 3)

γ= -0.1881 , R^2= 0.9984 (from equation 4)

The results of the parameterizations by one parameter of equations (3) and (4) for Model C using mass mix ratio are:

k= 0.1485, R^2=0.9676 (from equation 3)

γ= -0.1908, R^2= 0.9991 (from equation 4)

From the results of the parametrisation of $gf_{mix}(RH)$ and RH using equations (3) and (4) on the data of tables 4a, 4b and 4c, it can be seen that the data fitted the equations very well because of the values of R^2. It can also be observed that hygroscopicity of the mixtures (k) and γ using γ-law, all increase with the increase in the concentrations of the soots and the water solubles. Based on Liu et. al., [54] the mixtures can be described as less-hygroscopic.

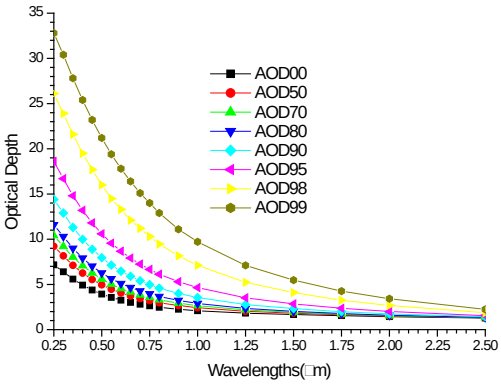

Figure 1a: A graph of optical depth against wavelengths for Model A.

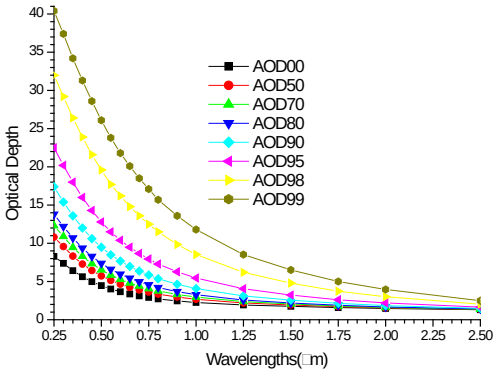

Figure 1b: A graph of optical depth against wavelengths for Model B.

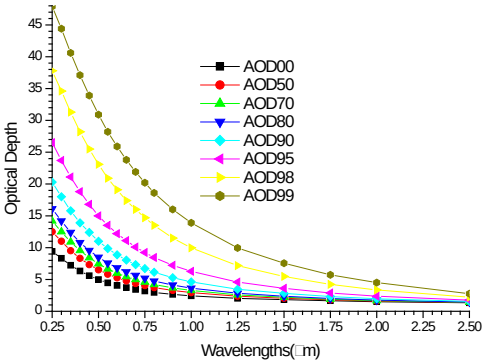

Figure 1c: A graph of optical depth against wavelengths for Model C.

From figures 1a, 1b and 1c, it can be observe that there is an increase in optical depth with the increase in RH and the concentrations of soots and water solubles and all satisfy the inverse power law.

The data that were used in plotting figures 1a, 1b and 1c were applied to equation (13), at the wavelengths of 0.25, 1.25 and 2.50 μm. The results obtained are as follows:

The relation between optical depth and RHs using equation (13) from the data of figure 1a for Model A. are:

At λ=0.25μ, A= 5.6518 , B= 1.2835, R^2= 0.6800

At λ=1.25 μ, A= 1.4139, B= 1.0407 , R^2= 0.5248

At λ=2.50 μ, A= 1.1537 , B= 0.3782 , R^2= 0.4122

The relation between optical depth and RHs using equation (13) from the data of figure 1b for Model B are:

At λ=0.25μ, A= 6.4792 , B= 1.3427, R^2= 0.6870

At λ=1.25 μ, A= 1.4693 , B= 1.1490 , R^2= 0.5386

At λ=2.50 μ, A= 1.1618 , B= 0.4407 , R^2= 0.4183

The relation between optical depth and RHs using equation (13) from the data of figure 1c for Model C are:

At λ=0.25μ, A= 7.3317 , B= 1.3832, R^2= 0.6939

At λ=1.25 μ, A= 1.5291 , B= 1.2377 , R^2= 0.5509

At λ=2.50 μ, A= 1.1670 , B= 0.5021 , R^2= 0.4243

From these relations between optical depth and RH which was obtained from the data used for plotting figures 1a, 1b and 1c, it shows decrease in R^2 and the exponent B with the increase in wavelength but shows increase with the increase in the concentrations of soot and water soluble. This shows that the relation is better for fine particles and the relation improves with the increase in the concentrations of fine particles (.soot and water soluble).

Table 5a the results of the Angstrom coefficients for Model A using equations (10), (11) and (12) at the respective relative humidities using regression analysis with SPSS16 for windows.

RH	Linear		Quadratic			Cubic			
(%)	R2	α	R2	α1	α2	R2	α1	α2	α3
0	0.9801	0.7839	0.9964	-0.7151	0.1499	0.9981	-0.7689	0.2114	0.0806
50	0.9902	0.8933	0.9968	-0.8439	0.1075	0.9991	-0.9152	0.1889	0.1067
70	0.9938	0.9431	0.9969	-0.9073	0.0780	0.9994	-0.9851	0.1667	0.1164
80	0.9961	0.9861	0.9971	-0.9646	0.0468	0.9996	-1.0463	0.1400	0.1222
90	0.9974	1.0608	0.9976	-1.0724	-0.0251	0.9998	-1.1553	0.0695	0.1240
95	0.9936	1.1267	0.9985	-1.1805	-0.1173	1.0000	-1.2526	-0.0351	0.1077
98	0.9805	1.1738	0.9996	-1.2852	-0.2425	1.0000	-1.3248	-0.1973	0.0592
99	0.9679	1.1750	0.9999	-1.3203	-0.3165	0.9999	-1.3324	-0.3027	0.0180

Table 5b the results of the Angstrom coefficients for Model B using equations (10), (11) and (12) at the respective relative humidities using regression analysis with SPSS16 for windows.

RH	Linear		Quadratic			Cubic			
(%)	R2	A	R2	α1	α2	R2	α1	α2	α3
0	0.9847	0.8447	0.9965	-0.7818	0.1370	0.9985	-0.8459	0.2102	0.0959
50	0.9932	0.9586	0.9968	-0.9191	0.0862	0.9993	-0.9990	0.1774	0.1196
70	0.9958	1.0091	0.9970	-0.9849	0.0527	0.9996	-1.0697	0.1495	0.1268
80	0.9971	1.0517	0.9973	-1.0434	0.0181	0.9997	-1.1303	0.1172	0.1300
90	0.9967	1.1235	0.9979	-1.1505	-0.0589	0.9999	-1.2341	0.0364	0.1249
95	0.9912	1.1825	0.9988	-1.2532	-0.1538	1.0000	-1.3206	-0.0769	0.1008
98	0.9768	1.2167	0.9997	-1.3437	-0.2764	1.0000	-1.3739	-0.2421	0.0451
99	0.9640	1.2086	0.9999	-1.3674	-0.3457	0.9999	-1.3691	-0.3438	0.0025

Table 5c the results of the Angstrom coefficients for Model C using equations (10), (11) and (12) at the respective relative humidities using regression analysis with SPSS16 for windows.

RH	Linear		Quadratic			Cubic			
(%)	R2	α	R2	α1	α2	R2	α1	α2	α3
0	0.9879	0.8962	0.9965	-0.8392	0.1241	0.9988	-0.9114	0.2064	0.1079
50	0.9950	1.0129	0.9969	-0.9824	0.0663	0.9995	-1.0682	0.1641	0.1282
70	0.9968	1.0631	0.9972	-1.0496	0.0295	0.9997	-1.1386	0.1311	0.1331
80	0.9974	1.1047	0.9975	-1.1082	-0.0077	0.9998	-1.1977	0.0945	0.1339
90	0.9956	1.1729	0.9982	-1.2131	-0.0877	0.9999	-1.2952	0.0059	0.1227
95	0.9890	1.2255	0.9991	-1.3097	-0.1833	1.0000	-1.3719	-0.1123	0.0930
98	0.9738	1.2486	0.9999	-1.3876	-0.3026	1.0000	-1.4095	-0.2776	0.0328
99	0.9610	1.2331	0.9999	-1.4020	-0.3675	0.9999	-1.3952	-0.3752	-0.0101

From tables 5a, 5b and 5c, it can be observed that at each table there is an increase in α with the increase in RH and the concentrations of soot and water soluble, except at tables 5b and 5c where it decreases at 99% RH. This shows that increase in concentration of soot and water soluble decreases the delinquent point with the mixtures. The increase in α signifies the increase in mode size distributions as a result of the increase in RH and soot and water soluble. The decrease in α2 and becoming more negative with the increase in RH and soot and water soluble reflects the increase in the concentrations of small particles as a result of nucleation, accumulation and sedimentation. The cubic part signifies mode distributions as bi-modal.

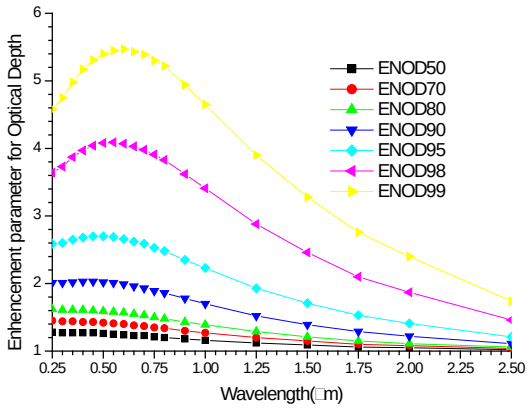

Figure 2a: A graph of enhancement parameter for optical depth against wavelengths for Model A.

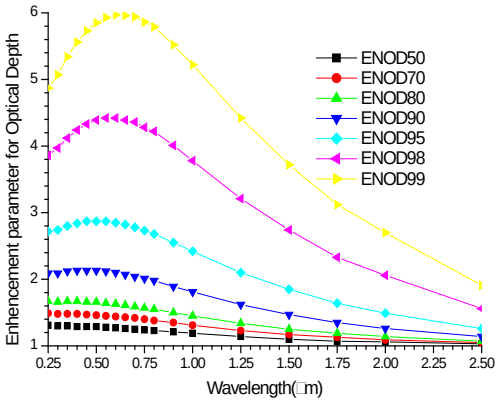

Figure 2b: A graph of enhancement parameter for optical depth against wavelengths for Model B

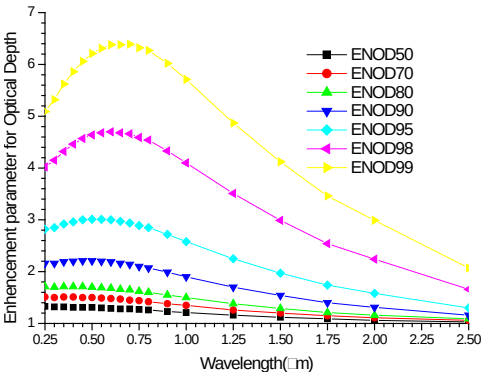

Figure 2c: A graph of enhancement parameter for optical depth against wavelengths Model C

Figures 2a, 2b and 2c show that the enhancement factors increase both with the increase in RH and concentrations of soot and water soluble in a non-linear form. Another interesting phenomena is the visible range window (0.4 - 0.7 µm) and near infrared (0.7-1.25 µm) where the enhancements are higher with both the increase in RH and the concentrations of soot and water soluble. This shows that increase in the concentrations of soot and water soluble together with the increase in RH can cause decrease in cloud cover, and/or reflective aerosol, decrease in global albedo, increase in energy input into Earth/Atmosphere system and finally can cause warming effect. That is it allows most solar radiation through to the surface and enables solar radiation to "deliver" the bulk of its energy to the surface (for use in climate processes).

The data used for plotting figures 2a, 2b and 2c were used on equations (7) and (8):

The results of the fitted curves of equations (7) and (8) for the data of figure 2a for Model A are presented as follows;

For a single parameter using equation (7).

At λ=0.25μ, γ= 0.9573, R^2= 0.9877

At λ=0.45μ, γ=1.0522 , R^2=0.9855

At λ=0.55 μ, γ=1.0643, R^2=0.9834

At λ=0.70 μ, γ=1.0408 , R^2=0.9810

At λ=1.25 μ, γ= 0.7741, R^2= 0.9775

At λ=2.50 μ, γ= 0.4264, R^2= 0.9044

For two parameters using equation (8).

At λ=0.25μ, a= 0.6421, b= -0.8407, R^2= 0.9550

At λ=0.45μ, a=0.9096 , b=-1.0218, R^2=0.9362

At λ=0.55 μ, a=0.9778 , b=-1.0569 , R^2=0.9295

At λ=0.70 μ, a=1.0087 , b=-1.0436 , R^2=0.9213

At λ=1.25 μ, a= 0.6734, b= -0.6888, R^2= 0.9013

At λ=2.50 μ, a= 0.0104, b= -0.1755, R^2= 0.8795

The results of the fitted curves of equations (7) and (8) for the data of figure 2b for Model B are presented as follows;

For a single parameter using equation (7).

At λ=0.25μ, γ= 1.0100, R^2= 0.9887

At λ=0.45μ, γ=1.1248 , R^2=0.9850

At λ=0.55 μ, γ=1.1453, R^2=0.9823

At λ=0.70 μ, γ=1.1314 , R^2=0.9794

At λ=1.25 μ, γ= 0.8560, R^2= 0.9776

At λ=2.50 μ, γ= 0.4520, R^2= 0.9201

For two parameters using equation (8).

At λ=0.25μ, a= 0.7029, b= -0.9095, R^2= 0.9550

At λ=0.45μ, a=0.9930 , b=-1.1223, R^2= 0.9362

At λ=0.55 μ, a=1.0723 , b=-1.1709 , R^2=0.9295

At λ=0.70 μ, a=1.1219 , b=-1.1737 , R^2= 0.9213

At λ=1.25 μ, a= 0.8380, b= -0.8111, R^2= 0.9013

At λ=2.50 μ, a= 0.0295, b= -0.2148, R^2= 0.8795

The results of the fitted curves of equations (7) and (8) for the data of figure 2c for Model C are presented as follows;

For a single parameter using equation (7).

At λ=0.25μ, γ= 1.0503, R^2= 0.9892

At λ=0.45μ, γ=1.1813 , R^2=0.9843

At λ=0.55 μ, γ=1.2100, R^2=0.9813

At λ=0.70 μ, γ=1.2056 , R^2=0.9777

At λ=1.25 μ, γ= 0.9284, R^2= 0.9764

At λ=2.50 μ, γ= 0.4761, R^2= 0.9323

For two parameters using equation (8).

At λ=0.25μ, a= 0.7461, b= -0.9620 , R^2= 0.9549

At λ=0.45μ, a=1.0525 , b=-1.2006, R^2=0.9361

At λ=0.55 μ, a=1.1402 , b=-1.2618 , R^2=0.9295

At λ=0.70 μ, a=1.2041 , b=-1.2801 , R^2=0.9213

At λ=1.25 μ, a= 0.9695 , b= -0.9195 , R^2= 0.9012

At λ=2.50 μ, a= 0.0592, b= -0.2525, R^2= 0.8799

The application of equations (7) and (8) to the data that was used to plot figures 2a, 2b and 2c are as follows: For single and two parameters, the values of γ and b increase respectively with the increase in the concentrations of soot and water soluble. The values are higher at the solar spectral window (0.4-0.7μm), observing the exponents (i.e γ and b), it can be seen that equation(7) is a direct power law while equaiton(8) is an inverse power law.

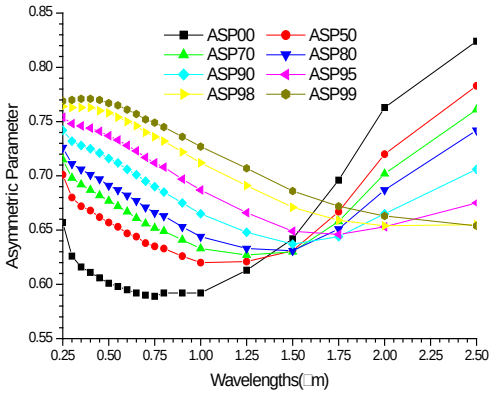

Figure 3a: A graph of Asymmetric parameter against wavelengths for Model A.

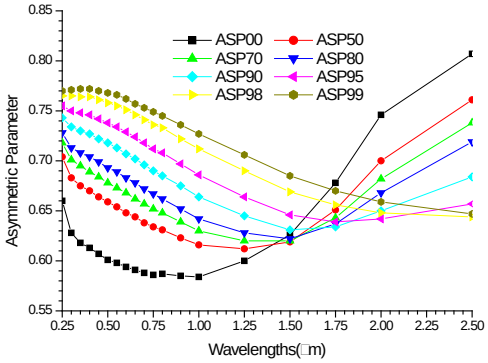

Figure 3b: A graph of Asymmetric parameter against wavelengths for Model B

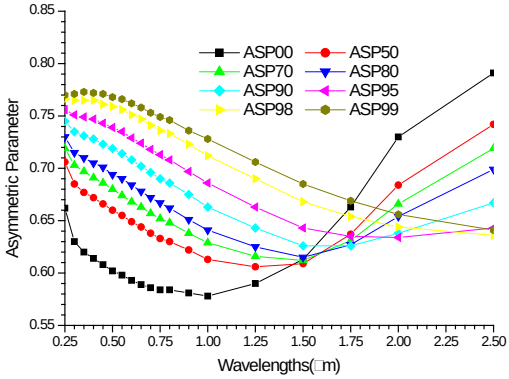

Figure 3c: A graph of Asymmetric parameter against wavelengths Model C

From figures 3a, 3b and 3c, there is an increase in the asymmetric parameter with the increase in RH and a slight increase of the asymmetric parameters with the increase in the concentration of soot and water soluble. The increase with the increase in RH is faster at the solar spectral window, this testifies the reason why equations (7) and (8) are higher at this spectral range.

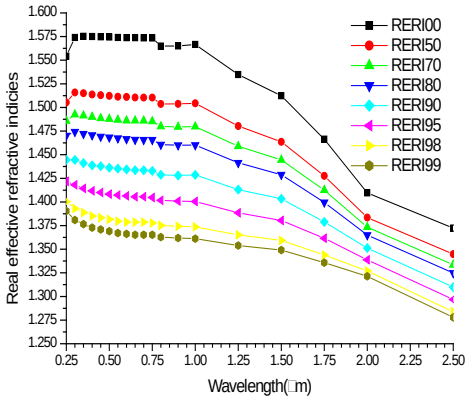

Figure 4a: A plot of real effective refractive indices against wavelength for Model A.

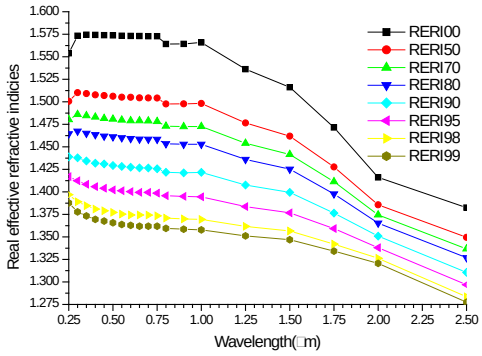

Figure 4b: A plot of real effective refractive indices against wavelength for Model B

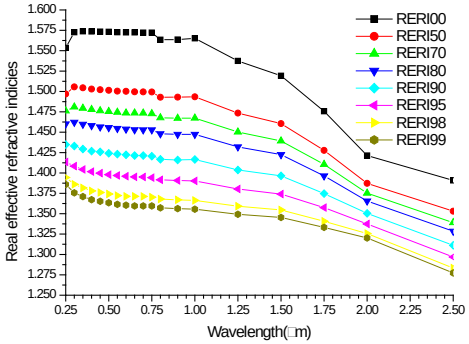

Figure 4c: A plot of real effective refractive indices against wavelength for Model C.

Figures 4a, 4b and 4c show that the real effective refractive indices decrease with increase in RH and soot and water soluble. The linear relation decreases with the increase in wavelength.

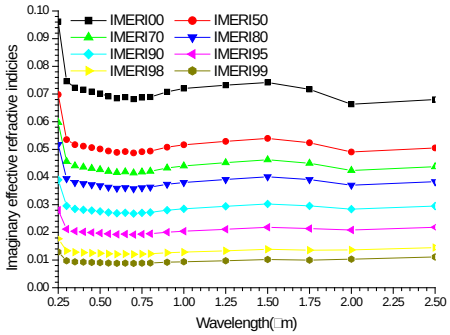

Figure 5a: A plot of imaginary effective refractive indices against wavelength for ModelA.

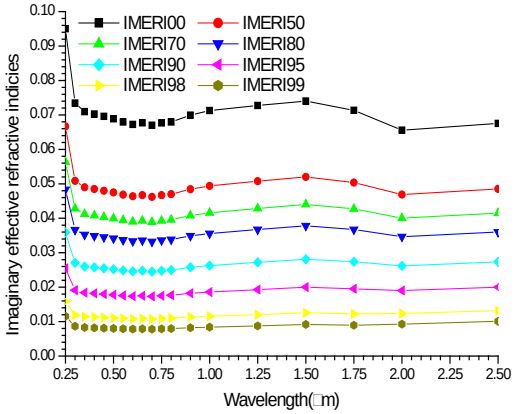

Figure 5b: A plot of imaginary effective refractive indices against wavelength for ModelB

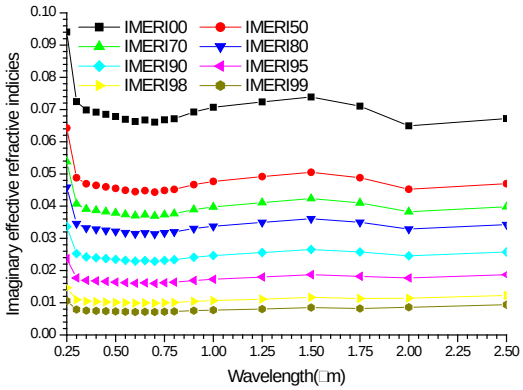

Figure 5c: A plot of imaginary effective refractive indices against wavelength for ModelC.

Figures 5a, 5b and 5c show there is a decrease in the imaginary effective refractive indices with the increase in RH and soot and water soluble. The plots becomes more linear with the increase in RH.

CONCLUSIONS

In this paper we investigated the influence of relative humidity and soot water soluble on the microphysical and optical properties of atmospheric aerosol mixtures. The principal conclusions are:

1) From the three $gf_{mix}(RH)$ it can be concluded that the higher values are observed using volume and mass mix ratios because of the high density of water soluble. This is in line with what Sheridan et al. [80] found, on the basis of analysis of in situ data collected at SGP in 1999, that aerosols containing higher fractions of smaller particles show larger hygroscopic growth factors. From our results despite soot being having the least size and higher in fractions, it shows that using volume mix and mass mix ratios, shows that the mixture is more hygroscopic. However, still in their studies, they also showed that aerosols containing higher fractions of more strongly absorbing particles exhibit lower hygroscopic growth factors, in our own case it shows that using number mix ratio. The importance of determining $gf_{mix}(RH)$ as a function of RH and volume fractions, mass fractions and number fractions, and enhancement parameters as a function of RH and wavelengths can be potentially important because it can be used for efficiently representing aerosols-water interactions in global models.

2) Equation (3) with mass mix ratios has higher R^2 while equation (4) has higher values of R^2 using volume mix ratio. But since volume mix ratios gave higher values of $gf_{mix}(RH)$, k and γ, and the values of R2 are greater than 95%, it can be concluded that just as the optical effects of atmospheric aerosols are more closely related to their volume than their number [85,86], we discovered that the microphysical properties are also more closely related to their volume followed by mass. The increase in the values of $gf_{mix}(RH)$, k and γ with the increase in soot and water soluble concentration show that they increase hygroscopicity of aerosols.

3) Changes in RH and soot and water soluble concentrations modified the optical properties not only of hygroscopic aerosol mixtures but also of mixtures containing non-hygroscopic aerosols like black carbon. As a result of wetting the hydroscopic particles grow, thereby changing the effective radius of the aerosol mixture and subsequently the aerosol extinction or aerosol optical thickness [87]. The changes are more substantial especially at the delinquent points where the hygroscopic growth factor, optical parameters and enhancement parameters increase so substantial that the process become strongly nonlinear with relative humidity [81,82,87]. This effect is observed at different wavelengths, but for higher RH, the increase in optical depth values is more evident at smaller wavelengths than longer wavelengths.

4) The observed variations in Angstrom coefficients can be explained by changes in the effective radius of a mixture resulting from changes in RH and/or soot and water soluble concentrations: the larger the number of small aerosol particles, the smaller the effective radius and the larger the Angstrom coefficient. As a consequence of non-uniform increase in the optical depth with the increase in RH, the Ångström coefficient also becomes a function of RH, though at the delinquent points it decreases with the increase in RHs. This is because at the delinquent conditions the hygroscopic aerosols particles grow and this is what makes the Angstrom coefficients to decrease. However, the change in Angstrom coefficient due to variation in RH is more than that caused by differences in soot concentrations.

5) The effect of RHs on asymmetric parameter shows that for smaller particles the hygroscopic growth increase forward scattering while for coarse particle it decreases forward scattering. It shows that increase in RH increases forward scattering because particle growth enhances forward diffraction Liou, [83] for smaller particles

while in larger particles it causes increase in the backward scattering. It also shows that the mixture is internally mixed for smaller particles because of the increase in forward scattering as a result of the hygroscopic growth [84].
6) These hygroscopic growth behaviors also reveal an immense potential of light scattering enhancement in the forward direction at high humidities and the potential for being highly effective cloud condensation nuclei for smaller particles.
7) Finally, the data fitted our models very and can be used to extrapolate the hygroscopic growth and enhancements parameters at any RH. The values of R^2 from the models show that Kelvin effects can be neglected.

REFERENCES

[1] Penner, J.E., et al., (1994). Quantifying and minimizing uncertainty of climate forcing by anthropogenic aerosols. Bulletin of the American Meteorological Society 75, 375–400.

[2] IPCC (2001): Climate Change 2001: The Scientific Basis. Houghton et al., Eds., Cambridge University Press, New York. 896 pp.

[3] Carrico, C. M., Kus, P., Rood, M. J., et al.: Mixtures of pollution, dust, sea salt, and volcanic aerosol during ACE-Asia: Radiative properties as a function of relative humidity, J. Geophys. Res., 108(D23), 8650, doi:10.1029/2003JD003405, 2003.

[4] Ogren, J. A. and Charlson R. J.: Implications for models and measurements of chemical inhomogeneities among cloud droplets, Tellus, 44B, 489–504, 1992.

[5] Hegg, D. A.: The importance of liquid phase oxidation of SO2 in the atmosphere, J. Geophys. Res., 90, 3773–3779, doi:10.1029/JD090iD02p03773, 1985.

[6] Blando, J. D. and Turpin, B. J.: Secondary organic aerosol formation in cloud and fog droplets: a literature evaluation of plausibility, Atmos. Environ., 34, 1623–1632, doi:10.1016/S1352-2310(99)00392-1, 2000.

[7] El Haddad, I., Yao Liu, Nieto-Gligorovski, L., Michaud, V., Temime-Roussel, B., Quivet, E., Marchand, N., Sellegri, K., and Monod, A.: In-cloud processes of methacrolein under simulated conditions – Part 2: Formation of secondary organic aerosol, Atmos. Chem. Phys., 9, 5107–5117, doi:10.5194/acp-9-5107-2009, 2009.

[8] Bateman, A. P., Nizkorodov, S. A., Laskin, J., and Laskin, A.: Photolytic processing of secondary organic aerosols dissolved in cloud droplets, Phys. Chem. Chem. Phys., 13, 12199–12212, doi:10.1039/c1cp20526a, 2011.

[9] Ervens, B., Turpin, B. J., and Weber, R. J.: Secondary organic aerosol formation in cloud droplets and aqueous particles (aqSOA): a review of laboratory, field and model studies, Atmos. Chem. Phys., 11, 11069–11102, doi:10.5194/acp-11-11069-2011, 2011.
[10] Orr Jr. C., Hurd F. K., Corbett W. J., 1958, Aerosol size and relative humidity, J. Colloid Sci., 13, 472–482.

[11] Tang I. N., (1976), Phase transformation and growth of aerosol particles composed of mixed salts, J. Aerosol Sci., 7, 361–371.

[12] Swietlicki, E., Hansson, H.-C., Hameri, K., Svenningsson, B., Massling, A., et al.: Hygroscopic properties of submicrometer atmospheric aerosol particles measured with H-TDMA instru-ments in various environments – a review, Tellus B, 60(3), 432–469, 2008.

[13] Corrigan, C. E. and Novakov, T.: Cloud condensation nucleus activity of organic compounds: a laboratory study, Atmos. Environ., 33 (17), 2661–2668, 1999.

[14] Pitchford, M. L. and Mcmurry, P. H.: Relationship between Measured Water-Vapor Growth and Chemistry of Atmospheric Aerosol for Grand-Canyon, Arizona, in Winter 1990, Atmos. Environ., 28 (5), 827–839, 1994.

[15] Shulman, M. L., Jacobson, M. C., Charlson, R. J., Synovec, R. E., and Young, T. E.: Dissolution behavior and surface tension effects of organic compounds in nucleating cloud droplets (vol. 23, p. 277, 1996), Geophys. Res. Lett., 23 (5), 603–603, 1996.

[16] Swietlicki, E., Zhou, J. C., Berg, O. H., Martinsson, B. G., Frank, G., Cederfelt, S. I., Dusek, U., Berner, A., Birmili, W., Wiedensohler, A., Yuskiewicz, B., and Bower, K. N.: A closure study of sub-micrometer aerosol particle hygroscopic behaviour, Atmos. Res., 50 (3-4), 205–240, 1999.

[17] Martin, S. T., Hung, H. M., Park, R. J., Jacob, D. J., Spurr, R. J. D., Chance, K. V., and Chin, M.: Effects of the physical state of tropospheric ammonium-sulfate-nitrate particles on global aerosol direct radiative forcing, Atmos. Chem. Phys., 4, 183–214, 2004, SRef-ID: 1680-7324/acp/2004-4-183.

[18] IPCC (2007). Climate Change 2007: The Scientific Basis. In Solomon, S., Ding, Y., Griggs, D.G., Noguer, M., Vanderlinden, P.G., Dai, X., Maskell, K. and Johnson, C.A. (Eds). Contribution of Working Group I to the Fourth Assessment Report of the Intergovernmental Panel on Climate Change. Cambridge University Press. Cambridge.

[19] Li, W.F, Bai, Z.P., Liu, A.X., Chen, J. and Chen, L. (2009). Characteristics of Major PM2.5Components during Winter in Tianjin, China. Aerosol Air Qual. Res. 9: 105–119.

[20] Shen, Z.X., Cao, J.J, Tong, Z., Liu, S.X., Reddy, L.S.S., Han, Y.M, Zhang, T. and Zhou, J. (2009). Chemical Characteristics of Submicron Particles in Winter in Xi'an. Aerosol Air Qual. Res. 9: 80–93.

[21] Hand, J. L. and Malm, W. C.: Review of the IMPROVE Equation for Estimating Ambient Light Extinction Coefficients-Final Report, 47, 2006.

[22] Wang, J., Hoffmann, A.A., Park, R.J., Jacob, D.J. and Martin, S.T. (2008a). Global Distribution of Solid and Aqueous Sulfate Aerosols: Effect of the Hysteresis of Particle Phase Transitions. J. Geophys. Res. 113: D11206. doi:10.1029/2007JD009367

[23] Wang, J., Jacob, D.J. and Martin S.T. (2008b). Sensitivity of Sulfate Direct Climate Forcing to the Hysteresis of Particle Phase Transitions. J. Geophys. Res. 113: D11207. doi: 10.1029/2007JD009368.

[24] Hansson, H.-C.; Rood, M. J.; Koloutsou-Vakakis, S.; Ha ¨meri, K.; Orsini, D.; Wiedensohler, A. NaCl aerosol particle hygroscopicity dependence on mixing with organic compounds. J. Atmos. Chem. 1998, 31(3), 321 -346.

[25] Cruz, C. N.; Pandis, S. N. Deliquenscence and hygroscopic growth of mixed inorganic-organic atmospheric aerosol. Environ. Sci. Technol. 2000, 34, 4313 -4319.

[26] Peng, C.; Chan, C. K. The water cycles of water-soluble organic salts of atmospheric importance. Atmos. Environ. 2001, 35, 1183-1192.

[27] Prenni, A. J.; DeMott, P. J.; Kreidenweis, S. M. Water uptake of internally mixed particles containing ammonium sulfate and dicarboxylic acids. Atmos. Environ . 2003, 27, 4243 -4251.

[28] Brooks, S. D.; DeMott, P. J.; Kreidenweis, S. M. Water uptake by particles containing humic materials and mixtures of humic materials with ammonium sulfate. Atmos. Environ. 2004, 38, 1859-1868.

[29] Badger, C. L.; George, I.; Griffiths, P. T.; Braban, C. F.; Cox, R. A.; Abbatt, J. P. D. Phase transitions and hygroscopic growth of aerosol particles containing humic acid and mixtures of humic acid and ammonium sulphate. Atmos. Chem. Phys . 2005, 6, 755 -768.

[30] Lee, Y. S.; Collins, D. R.; Li, R.; Bowman, K. P.; Feingold, G. Expected impact of an aged biomass burning aerosol on cloud condensation nuclei and cloud droplet concentrations. J. Geophys. Res.2006, 111 , D22204, doi:10.1029/2005JD0064.

[31] Hameri, K.; Vakeva, M.; Aalto, P. P.; Kulmala, M.; Swietlicki, E.; Zhou, J.; Seidl, J. W.; Becker, E.; O'Dowd, D. Hygroscopic and CCN properties of aerosol particles in boreal forests. Tellus, Ser. B 2001, 53B , 359-379.

[32] Randall, D. A., Wood, R. A., Bony, S., Colman, R., Fichefet, T., Fyfe, J., Kattsov, V., Pitman, A., Shukla, J., Srinivasan, J., Stouf-fer, R. J., Sumi, A., and Taylor, K. E.: Contribution of Working Group I to the Fourth Assessment Report of the Intergovernmen-tal Panel on Climate Change – Climate Models and their Evalua-tion, Cambridge University Press, Cambridge, United Kingdom and New York, 589–662, 2007.

[33] Kammermann, L., Gysel, M., Weingartner, E., and Baltensperger, U.: 13-month climatology of the aerosol hygroscopicity at the free tropospheric site Jungfraujoch (3580 m a.s.l.), Atmos. Chem. Phys., 10, 10717–10732, doi:10.5194/acp-10-10717-2010, 2010.

[34] Pahlow, M., Feingold, G., Jefferson, A., Andrews, E., Ogren, J. A., Wang, J., Lee, Y.-N., Ferrare, R. A., and Turner, D. D.: Comparison between lidar and nephelometer measurements of aerosol hygroscopicity at the Southern Great Plains Atmospheric Radiation Measurement site, J. Geophys. Res., 111, D005S15, doi:10.1029/2004JD005646, 2006.

[35] Kim, J., Yoon, S. C., Jefferson, A., et al.: Aerosol hygroscopic properties during Asian dust, pollution, and biomass burning episodes at Gosan, Korea in April 2001, Atmos. Environ., 40(8), 1550–1560, 2006.

[36] Schmidhauser, R., Zieger, P., Weingartner, E., Gysel, M., DeCarlo, P. F., and Baltensperger, U: Aerosol light scattering at high relative humidity at a high alpine site (Jungfraujoch), Euro-pean Aerosol Conference, Karlsruhe, Germany, 6–11 September 2009, T047A07, 2009.

[37] Fierz-Schmidhauser, R., Zieger, P., Vaishya, A., Monahan, C., Bialek, J., O'Dowd, C. D., Jennings, S. G., Baltensperger, U., and Weingartner, E.: Light scattering enhancement factors in the marine boundary layer (Mace Head, Ireland), J. Geophys. Res., 115, D20204,doi:10.1029/2009JD013755, 2010a.

[38] Fierz-Schmidhauser, R., Zieger, P., Gysel, M., Kammermann, L., DeCarlo, P. F., Baltensperger, U., and Weingartner, E.: Measured and predicted aerosol light scattering enhancement factors at the high alpine site Jungfraujoch, Atmos. Chem. Phys., 10, 2319–2333,doi:10.5194/acp-10-2319-2010, 2010b.

[39] Zieger, P., Weingartner, E., Henzing, J., Moerman, M., de Leeuw, G., Mikkila, J., Ehn, M., Petaja, T., Clemer, K., van Roozen-dael, M., Yilmaz, S., Frieß, U., Irie, H., Wagner, T., Shaigan-far, R., Beirle, S., Apituley, A., Wilson, K., and Baltensperger, U. (2011): Comparison of ambient aerosol extinction coefficients ob-tained from in-situ, MAX-DOAS and LIDAR measurements at Cabauw, Atmos. Chem. Phys., 11, 2603–2624,doi:10.5194/acp-11-2603-2011.

[40] Yan, P., Pan, X. L., Tang, J., Zhou, X. J., Zhang, R. J., and Zeng, L. M.: Hygroscopic growth of aerosol scattering coeffi-cient: a comparative analysis between urban and suburban sites at winter in Beijing, Particuology, 7, 52–60, 2009.

[41] Fitzgerald, J. W., Hoppel, W. A., and Vietti, M. A.: The size and scattering coefficient of urban aerosol particles at Washington, DC as a function of relative humidity, J. Atmos. Sci., 39, 1838–1852, 1982.

[42] Jeong M. J, Li Z., Andrews E., Tsay S. C., (2007) Effect of aerosol humidification on the column aerosol optical thickness over the Atmospheric Radiation Measurement Southern Great Plains site, J. Geophys. Res., 112, D10202, doi:10.1029/2006JD007176.

[43] Rapti A.S., (2005) Spectral optical atmospheric thickness dependence on the specific humidity in the presence of continental and marine air masses, Atmos. Res., 78(1–2),13–32.

[44] Hess M., Koepke P., and Schult I (May 1998), Optical Properties of Aerosols and Clouds: The Software Package OPAC, Bulletin of the A merican Met. Soc. 79, 5, p831-844.

[45] Randles , C. A. , Russell L. M. and. Ramaswamy V. (2004) Hygroscopic and optical properties of organic sea salt aerosol and consequences for climate forcing, Geophysical Research Letters, Vol. 31, L16108, doi:10.1029/2004GL020628.

[46] Sjogren, S., Gysel, M., Weingartner, E., Baltensperger, U., Cubi-son, M. J., Coe, H., Zardini, A. A., Marcolli, C., Krieger, U. K., and Peter, T.: Hygroscopic growth and water uptake kinetics of two-phase aerosol particles consisting of ammonium sulfate, adipic and humic acid mixtures, J. Aerosol Sci., 38, 157–171, doi:10.1016/j.jaerosci.2006.11.005, 2007.

[47] Stokes, R. H. and Robinson, R. A.: Interactions in aqueous nonelec-trolyte solutions. I. Solute-solvent equilibria, J. Phys. Chem., 70, 2126–2130, 1966.

[48] Meyer, N. K., Duplissy, J., Gysel, M., Metzger, A., Dommen, J., Weingartner, E., Alfarra, M. R., Prevot, A. S. H., Fletcher, C., Good, N., McFiggans, G., Jonsson,˚ A. M., Hallquist, M., Baltensperger, U., and Ristovski, Z. D.: Analysis of the hy-groscopic and volatile properties of ammonium sulphate seeded and unseeded SOA particles, Atmos. Chem. Phys., 9, 721–732, doi:10.5194/acp-9-721-2009, 2009.

[49] Stock M., Y. F. Cheng, W. Birmili, A. Massling, B. Wehner, T. Muller, S. Leinert, N. Kalivitis,N. Mihalopoulos, and A. Wiedensohler, Hygroscopic properties of atmospheric aerosol particles over the Eastern Mediterranean: implications for regional direct radiative forcing under clean and polluted conditions, Atmos. Chem. Phys., 11, 4251–4271, 2011 www.atmos-chem-phys.net/11/4251/2011/ doi:10.5194/acp-11-4251-2011

[50] Duplissy J., P. F. DeCarlo, J. Dommen, M. R. Alfarra, A. Metzger, I. Barmpadimos, A. S. H. Prevot, E. Weingartner, T. Tritscher, M. Gysel, A. C. Aiken, J. L. Jimenez, M. R. Canagaratna , D. R. Worsnop, D. R. Collins, J. Tomlinson, and U. Baltensperger, (2011) Relating hygroscopicity and composition of organic aerosol particulate matter Atmos. Chem. Phys., 11, 1155–1165, www.atmos-chem-phys.net/11/1155/2011/ doi:10.5194/acp-11-1155-2011.

[51] Meier J., B. Wehner, A. Massling,*, W. Birmili, A. Nowak, T. Gnauk, E. Br¨ uggemann, H. Herrmann, H. Min, and A. Wiedensohler Hygroscopic growth of urban aerosol particles in Beijing (China) during wintertime: a comparison of three experimental methods, Atmos. Chem. Phys., 9, 6865–6880, 2009 www.atmos-chem-phys.net/9/6865/2009/

[52] Petters, M. D. and Kreidenweis, S. M. (2007). A single parameter representation of hygroscopic growth and cloud condens ation nucleus activity. Atmos. Chem. Phys. 7(8): 1961–1971.

[53] Christensen, S. I. and Petters, M. D. (2012). Th e role of temperature in cloud droplet activation. J. Phys. Chem. A 116(39): 9706–9717.

[54] Liu P. F., Zhao C. S., Gobel T., Hallbauer E., Nowak A., Ran L., Xu W. Y., Deng Z. Z., Ma N., Mildenberger K., Henning S., Stratmann F., and Wiedensohler A. (2011) Hygroscopic proper ties of aerosol par ticles at high relative humidity and their diurnal variations in the Nor th China Plain, Atmos. Chem. Phys. Discuss., 11, 2991–3040

[55] Swietlicki, E., Zhou, J., Covert, D. S., H¨ameri, K., Busch, B., V¨akeva, M., Dusek, U., Berg, O. H., Wiedensohler, A., Aalto, P., M¨akel¨a, J., Martinsson, B. G., Papaspiropoulos, G., Mentes, B., Frank, G., and Stratmann, F.: Hygroscopic properties of aerosol particles in the northeastern Atlantic during ACE-2, Tellus, 52B, 201–227, 2000.

[56] Birmili, W., Nowak, A., Schwirn, K., Lehmann, K.et al. (2004) A new method to accurately relate dry and humidified number size distributions of atmospheric aerosols. Journal of Aerosol Science 1, 15–16, Abstracts of EAC, Budapest 2004.

[57] Kasten, F.: Visibility forecast in the phase of pre-condensation, Tel-lus, XXI, 5, 631–635, 1969.

[58] Gysel, M., McFiggans, G. B., and Coe, H.: Inversion of tandem differential mobility analyser (TDMA) measurements, J. Aerosol Sci., 40, 134–151, 2009.

[59] Putaud, J. P. (2012): Interactive comment on “Aerosol hygroscopicity at Ispra EMEP-GAW station” by M. Adam et. al., Atmos. Chem. Phys. Discuss., 12, C1316–C1322.

[60] Doherty, et al., 2005. A comparison and summary of aerosol optical properties as observed in situ from aircraft, ship, and land during ACE-Asia. Journal of Geophysical Research 110, D04201.

[61] Quinn, P. K., et al. (2005) , Impact of particulate organic matter on the relative humidity dependence of light scattering: A simplified parameterization, Geophys. Res. Lett., 32, L22809, doi:10.1029/2005GL024322.

[62] Gasso S., et al. (2000), Influence of humidity on the aerosol scattering coefficient and its effect on the upwelling radiance during ACE-2, Tellus, Ser. B , 52, 546 – 567.

[63] Clarke, A., et al. (2007), Biomass burning and pollution aerosol over North America: Organic components an d their influence on spectral optical properties and humidification response, J. Geophys. Res., 11 2, D12S18, doi:10.1029/2006JD007777.

[64] Hanel, G. (1976). The Properties of Atmospheric Aerosol Particles as Functions of Relative Humidity at Thermodynamic Equilibrium with Surrounding Moist Air. InAdvances in Geophysics, Vol. 19 , H. E. Landsberg and J. Van Mieghem, eds., Academic Press, New York, pp. 73–188.

[65] Angstrom, A.(1961): Techniques of Determining the Turbidity of the At-mosphere, Tellus, 13, 214–223.

[66] King, M. D. and Byrne, D. M.: A method for inferring total ozone content from spectral variation of total optical depth obtained with a solar radiometer, J. Atmos. Sci., 33, 2242–2251, 1976.

[67] Eck, T. F., Holben, B. N., Reid, J. S., Dubovic, O., Smirnov, A., O’Neil, N. T., Slutsker, I., and Kinne, S.: Wavelength dependence of the optical depth of biomass burning, urban, and desert dust aerosols, J. Geophys. Res., 104(D24), 31 333–31 349, 1999.

[68] Eck, T. F., Holben, B. N., Dubovic, O., Smirnov, A., Slutsker, I., Lobert, J. M., and Ramanathan, V.: Column-integrated aerosol optical properties over the Maldives during the northeast mon-soon for 1998–2000, J. Geophys. Res., 106, 28 555–28 566, 2001a.

[69] Eck, T. F., Holben, B. N., Ward, D. E., Dubovic, O., Reid, J. S., Smirnov, A., Mukelabai, M. M., Hsu, N. C., O' Neil, N. T., and Slutsker, I.: Characterization of the optical properties of biomass burning aerosols in Zambia during the 1997 ZIBBEE field campaign, J. Geophys. Res., 106(D4), 3425–3448, 2001b.

[70] Kaufman, Y. J., Aerosol optical thickness and atmospheric path radiance, J. Geophys. Res., 98, 2677-2992, 1993.

[71] O'Neill, N. T., Dubovic, O., and Eck, T. F.(2001): Modified˚ Angstr¨ om exponent for the characterization of submicrometer aerosols, Appl. Opt., 40(15), 2368–2375.

[72] O'Neill, N. T., Eck, T. F., Smirnov, A., Holben, B. N., and Thulasiraman, S.: Spectral dis-crimination of coarse and fine mode optical depth, J. Geophys. Res., 198(D17), 4559, doi:101029/2002JD002975, 2003.

[73] Pedros, R., Martinez-Lozano, J. A., Utrillas, M. P., Gomez-Amo, J. L., and Tena, F.(2003): Column-integrated aerosol, optical properties from ground-based spectroradiometer measurements at Barrax (Spain) during the Digital Airborne Imaging Spectrometer Experiment (DAISEX) campaigns, J. Geophys. Res., 108(D18), 4571, doi:10.1029/2002JD003331.

[74] Kaskaoutis, D. G. and Kambezidis, H. D.(2006): Investigation on the wavelength dependence of the aerosol optical depth in the Athens area, Q. J. R. Meteorol. Soc., 132, 2217–2234.

[75] Schmid, B., Hegg, D.A., Wang, J., Bates, D., Redemann, J., Russell, P.B., Livingston, J.M., Jonsson, H.H., Welton, E.J., Seinfeld, J.H., Flagan, R.C., Covert, D.S., Dubovik, O., Jefferson, A., (2003). Column closure studies of lower tropospheric aerosol and water vapor during ACE-Asia using airborne Sun photometer and airborne in situ and ship-based lidar measurements. Journal of Geophysical Research 108 (D23), 8656.

[76] Martinez-Lozano, J.A., Utrillas, M.P., Tena, F., Pedros, R., Canada, J., Bosca, J.V., Lorente, J., (2001). Aerosol optical characteristics from summer campaign in an urban coastal Mediterranean area. IEEE Transactions on Geoscience and Remote Sensing 39, 1573–1585.

[77] Aspens D. E. (1982), Local-field effect and effective medium theory: A microscopic perspective Am. J. Phys. 50, 704-709.

[78] Lorentz, H. A. (1880). Ueber die Beziehung zwischen der Fortpflanzungsgeschwindigkeit des Lichtes und der Korperdichte. Ann. P hys. Chem. 9, 641–665.

[79] Lorenz, L. (1880). Ueber die Refractionconstante. A nn. P hys. Chem. 11, 70–103.

[80] Sheridan, P. J., Delene D. J., and Ogren J. A. (2001), Four years of con-tinuous surface aerosol measurements from the Department of Energy's Atmospheric Radiation Measurement Program Southern Great Plains Cloud and Radiation Testbed site, J. Geophys. Res. , 106 , 20,735 – 20,747.

[81] Fitzgerald , J. W. (1975) Approximation formulas for the equilibrium size of an aerosol particle as a function of its dry size and composition and ambient relative humidity. J. Appl . Meteorol. , 14, 1044 –1049.

[82] Tang I.N., (1996) Chemical and size effects of hygroscopic aerosols on light scattering coefficient, J. Geophys. Res., 101(D14),19245–19250.

[83] Liou, K. N. (2002), An Introduction ro Atmospheric Radiation, 583pp., Elsevier, New York.

[84] Wang, J., and S. T. Martin (2007), Satellite characterization of urban aerosols: Importance of including hygroscopicity and mixing state in the retrieval algorithms, J. Geophys. Res., 112 , D 17203, doi:1 0.1029 /2006JD008078.

[85] Whitby, K. (1978), The physical characteristics of sulfur aerosols, Atmos. Environ., 12, 135–159.

[86] Seinfeld, J., and S. Pandis (1998), Atmospheric Chemistry and Physics: From Air Pollution to Climate Change, Wiley.

[87] Kuśmierczyk-Michulec, J. (2009). Ångström coefficient as an indicator of the atmospheric aerosol type for a well- mixed atmospheric boundary layer: Part 1: Model development. Oceanologia , Vol. 51, p. 5-39.